Received: 12 August 2022 | Revised: 21 November 2022 | Accepted: 12 December 2022

DOI: 10.1002/psp4.12910

ARTICLE

Model-based prediction of effective target exposure for MEN1611 in combination with trastuzumab in HER2-positive advanced or metastatic breast cancer patients

Elena M. Tosca[1] | **Elisa Borella**[2] | **Chiara Piana**[2] | **Salim Bouchene**[2] | **Giuseppe Merlino**[3] | **Alessio Fiascarelli**[3] | **Paolo Mazzei**[2] | **Paolo Magni**[1]

[1]Laboratory of Bioinformatics, Mathematical Modelling and Synthetic Biology, Department of Electrical, Computer and Biomedical Engineering, Università degli Studi di Pavia, Pavia, Italy

[2]Clinical Pharmacology Department, Menarini Stemline, Florence, Italy

[3]Experimental and Translational Oncology Department, Menarini Stemline, Pomezia, Italy

Correspondence
Paolo Magni, Laboratory of Bioinformatics, Mathematical Modelling and Synthetic Biology, Department of Electrical, Computer and Biomedical Engineering, Università degli Studi di Pavia, via Ferrata 5, Pavia (PV) 27100, Italy.
Email: paolo.magni@unipv.it

Present address
Salim Bouchene, Pumas-AI, Inc., Paris, France

Abstract

MEN1611 is a novel orally bioavailable PI3K inhibitor currently in clinical development for patients with HER2-positive (HER2+) PI3KCA mutated advanced/metastatic breast cancer (BC) in combination with trastuzumab (TZB). In this work, a translational model-based approach to determine the minimum target exposure of MEN1611 in combination with TZB was applied. First, pharmacokinetic (PK) models for MEN1611 and TZB in mice were developed. Then, in vivo tumor growth inhibition (TGI) data from seven combination studies in mice xenograft models representative of the human HER2+ BC non-responsive to TZB (alterations of the PI3K/AkT/mTOR pathway) were analyzed using a PK-pharmacodynamic (PD) TGI model for co-administration of MEN1611 and TZB. The established PK-PD relationship was used to quantify the minimum effective MEN1611 concentration, as a function of TZB concentration, needed for tumor eradication in xenograft mice. Finally, a range of minimum effective exposures for MEN1611 were extrapolated to patients with BC, considering the typical steady-state TZB plasma levels in patients with BC following three alternative regimens (i.v. 4 mg/kg loading dose +2 mg/kg q1w, i.v. 8 mg/kg loading dose +6 mg/kg q3w or s.c. 600 mg q3w). A threshold of about 2000 ng·h/ml for MEN1611 exposure associated with a high likelihood of effective antitumor activity in a large majority of patients was identified for the 3-weekly and the weekly i.v. schedule for TZB. A slightly lower exposure (i.e., 25% lower) was found for the 3-weekly s.c. schedule. This important outcome confirmed the adequacy of the therapeutic dose administered in the ongoing phase 1b B-PRECISE-01 study in patients with HER2+ PI3KCA mutated advanced/metastatic BC.

Study Highlights

WHAT IS THE CURRENT KNOWLEDGE ON THE TOPIC?

MEN1611 is a novel orally bioavailable PI3K inhibitor currently in clinical development for patients with HER2-positive advanced or metastatic breast cancer (BC) in combination with trastuzumab (TZB).

WHAT QUESTION DID THIS STUDY ADDRESS?

We aimed to develop a translational approach based on the pharmacokinetic-pharmacodynamic (PK-PD) modeling of preclinical data to determine the minimum target exposure of MEN1611 when co-administered with three alternative regimens of TZB (i.v. 4 mg/kg loading dose +2 mg/kg q1w, i.v. 8 mg/kg loading dose +6 mg/kg q3w or s.c. 600 mg q3w) in patients with BC.

WHAT DOES THIS STUDY ADD TO OUR KNOWLEDGE?

For each of the TZB regimen, a range for the effective MEN1611 exposure was identified. When TZB was administered i.v., MEN1611 exposure above 2000 ng·h/ml is expected to be associated with a high likelihood of effective antitumor activity in a large majority of patients. A slightly lower threshold (i.e., 25% lower) is found for the 3-weekly s.c. schedule.

HOW MIGHT THIS CHANGE DRUG DISCOVERY, DEVELOPMENT, AND/OR THERAPEUTICS?

This study confirms the adequacy of the therapeutic dose administered in the ongoing phase 1b B-PRECISE-01 study in patients with HER2-positive advanced or metastatic BC.

INTRODUCTION

Overexpression of human epidermal growth factor receptor 2 (HER2) occurs in up to 30% of breast cancers (BCs)[1] and is a marker of aggressive disease.[2] The development of HER2-targeted therapies significantly improved the survival outcome of patients with HER2-positive (HER2+) BC. Trastuzumab (TZB; Herceptin; Genentech) is the first HER2-targeted monoclonal antibody approved by the US Food and Drug Administration (FDA) for the treatment of metastatic HER2+ BC.[3] Despite the undeniable benefits of TZB for HER2+ BC treatment, the majority of patients exhibit primary or acquired resistance.[4–6] Aberrant activation of the phosphoinositide 3-kinase/protein kinase B/mammalian target of rapamycin (PI3K/Akt/mTOR) pathway has been recognized as one of the main drivers of TZB resistance. In particular, activating mutations in the gene encoding PI3K alpha catalytic subunit (PIK3CA) are found in ~40% of HER2+ BC and resulted associated with TZB insensitivity. Based on these findings, PI3K/Akt/mTOR pathway has become an attractive therapeutic target to overcome or prevent resistance to anti-HER2 treatment with TZB and several inhibitors of this pathway are under investigation in this disease setting.[4,7,8]

MEN1611 (CH5132799) is a potent, orally bioavailable, selective class I PI3K inhibitor[9] active on the p110α (mutant and wild type), β and γ isoforms, while sparing the δ isoform. MEN1611 resulted effective in a broad range of tumor types with demonstrated efficacy in HER2+ BC xenograft models, harboring PIK3CA mutations.[10] It was administered as single agent in a first-in-human (FIH) study at different doses and the maximum tolerated dose (MTD) of MEN1611 was determined to be 48 mg twice daily (b.i.d.).[11] Preclinical and clinical evidences, as well as literature data from other PI3K inhibitors, suggested that combining MEN1611 with TZB-based therapy could provide clinical benefits for TZB-insensitive patients and supported the rational to develop MEN1611 in combination with TZB for the treatment of HER2+ advanced/metastatic BC.[12] MEN1611 has been evaluated for this indication in an open-label, multicenter, phase Ib trial, namely B-PRECISE-01 study enrolling patients with PIK3CA mutated HER2+ advanced/metastatic BC which progressed after at least two lines of anti-HER2-based therapy, including TZB.[13]

The possibility to anticipate the pharmacologically active exposures for an anticancer drug combination during or before its clinical evaluation would allow to assess the potential therapeutic advantage and the adequacy of the clinical combination protocols, maximizing the probability of success of combination trials, and, more importantly, minimizing the number of patients receiving suboptimal combination treatments.

Several approaches to model preclinical data of oncology drugs are already available and successfully applied during the drug development process.[14–17] These approaches are generally based on pharmacokinetic-pharmacodynamic (PK-PD) modeling of tumor growth inhibition (TGI) observed in xenograft experiments after the administration of tested compounds in monotherapy[18–23] or combination regimens.[24–27] Their growing success is due to their ability to extract, summarize, and integrate results from in vivo experiments, in order to quantify drug activity, compare drug candidates, identify drug–drug interaction, and, most importantly, translate preclinical results into the clinical setting. Indeed, in some cases, high correlations between model-derived metrics of systemic exposure leading to TGI in xenograft models and clinically active exposures or doses in patients with cancer have been demonstrated.[28,29]

The present pharmacometric analysis aimed at developing a translational PK-PD model to predict from preclinical data a set of minimal effective MEN1611 exposures, when administered in combination with TZB in the B-PRECISE-01 patient population.

METHODS

A stepwise PK-PD modeling approach was used.[30] First PK models for MEN1611 and TZB were developed; then, in vivo TGI data from multiple combination studies in xenograft mice models representing human HER2+ BC nonresponsive to TZB were analyzed using a PK-PD TGI model for co-administration of MEN1611 and TZB. The established PK-PD relationship was used to quantify the minimum effective MEN1611 concentration, as a function of TZB concentration, needed for tumor eradication in xenograft mice models. Finally, the predicted range of minimum effective MEN1611 concentrations were extrapolated to B-PRECISE-01 patients, using the typical plasma levels of TZB in human for three alternative dosing regimens.

Experimental methods

Pharmacokinetic assessment

Data from two studies on tumor-bearing mice treated with different doses of TZB labeled with different radioisotopes were collected from literature.[31,32]

TZB-PK study 1[31]: severe combined immunodeficiency mice bearing KPL-4 tumor received a single intravenous (i.v.) administration of ^{111}In-TZB (10 μCi) and ^{125}I-TZB (5 μCi), along with 0.1, 1.4, and 17 mg/kg of unlabeled TZB (i.e., about 3.43, 32.68, and 383.68 μg of TZB for a typical mouse weighting 22.5 g). Blood was collected over 168 h postdose and percent of administered dose per gram of tissue (%ID/g) were provided for each sample.

TZB-PK study 2[32]: (nude) mice bearing SKOV3 tumor received 15 MBq (≈405 μCi) ^{86}Y-TZB (i.e., about 17.65 μg of TZB) intraperitoneally (i.p.). Relative activity concentration (%IA/g) were measured over 3 days postdose.

Data in %ID/g and %IA/g from TZB-PK Study 1 and 2 were converted into plasma mass concentration following the methodology reported in Material S1.

PK of MEN1611 after i.v. and oral (p.o.) administrations was characterized in two mice studies.

MEN1611-PK study 1: MEN1611 (solution – vehicle DMSO) was administered i.v. at 2 mg/kg and p.o. at 0.5, 1, 2, or 5 mg/kg to BALB-nu/nu mice (2 animals for i.v., and 4 animals/group for p.o.). For i.v. administration, the drug solution was injected into the tail vein whereas, for p.o. administration, the drug solution was administered into the stomach using a flexible feeding needle. Blood samples were collected over 24 h postdose.

MEN1611-PK study 2: MEN1611 (suspension – vehicle MCT) was given p.o. by gavage for 5 days at 1.25, 6.25, and 12.5 mg/kg to CD-1 mice (12 animals/group). Blood samples were collected over 24 h postdose on days 1 and 5. Average plasma concentration-time profiles were considered stratified by study, dose level, and administration day.

In vivo efficacy assessment of MEN1611 in combination with TZB

Seven in vivo combination TGI studies involving three cell-derived xenograft models and four patient-derived xenograft (PDX) models representative of human HER2+ BC (overexpression of HER2), TZB resistant and harboring PI3K pathway alterations were considered. The PIK3CA gene was mutated in six of the considered BC cell lines, whereas the PDX-173-JAL cell line harbored mutation of the PIK3CG gene (Table 1). All experiments were carried out in accordance with the Guideline for Accommodation and Care of Laboratory Animals and were approved by local ethical committee. Mice body weight (BW) and tumor sizes were measured and recorded every 3–4 days. Mice were euthanized when tumors reached a volume ~10% of total BW or when mice BW decreased by more than 20%, compared to the BW of mouse at the first day of treatment. Tumor sizes (i.e., the greatest longitudinal [length] and transverse [width] diameters), were measured by Vernier caliper. Tumor weight (TW) was calculated under the hypothesis of an oblate ellipsoidal shape through the formula[33,34]:

$$\mathrm{TW(g)} = \rho \frac{\mathrm{length\ (cm)} \cdot \mathrm{width}^2\ (\mathrm{cm}^2)}{2} \quad (1)$$

TABLE 1 Analyzed xenograft experiments evaluating combination of MEN1611 and TZB

TGI study	Tumor cell line	Cell line characteristics	Animals	Arm	No. of animals	Compound	Dose level (mg/kg)	Route	Regimen
A	KPL4	HER2 amp	BALB	Arm a_1	5	Vehicle	–	–	–
		PI3KCA mut	nu/nu mice	Arm a_2	5	MEN1611	12.5 mg/kg	p.o.	qdx12
		(H1047R)		Arm a_3	5	TZB	30 mg/kg	i.v.	q1w for 12 days
		TZB R		Arm a_4	5	MEN1611 + TZB	12.5 mg/kg + 30 mg/kg	p.o. i.v.	qdx12 + q1w for 12 days
B	JIMT-1	HER2 amp	CD-1 mice	Arm b_1	4	Vehicle	–	–	–
		PI3KCA mut		Arm b_2	5	MEN1611	6.5 mg/kg	p.o.	qdx12
		(C420R)		Arm b_3	6	TZB	30 mg/kg	i.p.	q1w for 2 weeks
		TZB R		Arm b_4	6	MEN1611 + TZB	6.5 mg/kg + 30 mg/kg	p.o. i.p.	qdx12 + q1w for 2 weeks
C	HCC1954	HER2 amp	CD-1 mice	Arm c_1	5	Vehicle	–	–	–
		PI3KCA mut		Arm c_2	5	MEN1611	6.5 mg/kg	p.o.	qdx12
		(H1047R)		Arm c_3	5	TZB	30 mg/kg	i.p.	q1w for 2 weeks
		TZB R		Arm c_4	6	MEN1611 + TZB	6.5 mg/kg + 30 mg/kg	p.o. i.p.	qdx12 + q1w for 2 weeks
D	CTG-0033 PDX	HER2 amp	Athymic	Arm d_1	7	Vehicle	–	–	–
		PI3KCA mut	nu/nu mice	Arm d_2	8	MEN1611	6.5 mg/kg	p.o.	qdx12
		(E545A)		Arm d_3	8	TZB	30 mg/kg	i.p.	q1w for 2 weeks
		TZB R		Arm d_4	8	MEN1611 + TZB	6.5 mg/kg + 30 mg/kg	p.o. i.p.	qdx12 + q1w for 2 weeks
E	BC-PDX-67	HER2 amp	NOD/SCID mice	Arm e_1	10	Vehicle	–	–	–
		PI3KCA mut		Arm e_2	10	MEN1611	6.5 mg/kg	p.o.	qdx12
		(K111E)		Arm e_3	9	TZB	10 mg/kg	i.p.	q2w for 2 weeks
		TZB R		Arm e_4	10	MEN1611 + TZB	6.5 mg/kg + 10 mg/kg	p.o. i.p.	qdx12 + q2w for 2 weeks
F	PDX-153	HER2 amp	Athymic	Arm f_1	7	Vehicle	–	–	–
		PI3KCA mut	nu/nu mice	Arm f_2	8	MEN1611	6.5 mg/kg	p.o.	qdx12
		(K111E)		Arm f_3	9	TZB	10 mg/kg	i.p.	q2w for 3 weeks
		TZB R		Arm f_4	9	MEN1611 + TZB	6.5 mg/kg + 10 mg/kg	p.o. i.p.	qdx12 + q2w for 3 weeks
G	PDX-173-JAL	HER2 amp	Athymic	Arm g_1	4	Vehicle	–	–	–
		ER amp	nu/nu mice	Arm g_2	9	MEN1611	6.5 mg/kg	p.o.	qd for 6 weeks
		PI3KCG mut		*arm* g_3	4	TZB	10 mg/kg	i.p.	q2w for 3 weeks
		TZB R		Arm g_4	6	MEN1611 + TZB	6.5 mg/kg + 10 mg/kg	p.o., i.p.	qd for 6 weeks +q2w for 3 weeks

Abbreviations: mut, mutated; TZB R, Trastuzumab resistant.

assuming unit density ($\rho = 1\,g/cm^3$) for tumor tissue. Where the average tumor volume reached 200–300 mm^3, animals were randomly assigned into four groups (1 control and 3 treatment arms; Table 1) to evaluate the anticancer effect of MEN1611 in combination with TZB. MEN1611 and TZB doses were selected based on translation of the expected human exposures at clinical doses into mice model. Control mice were administered with vehicle (DMSO/Cremophor EL, 50%/50% volumes, mixed solution) alone. Average TW time profiles stratified by studies and arms are reported in Figure 1, whereas individual data in Figures S1–S7 in the Material S2.

Pharmacokinetic modeling

Two-compartment disposition models with first-order absorption were used to describe the PK of TZB (i.v. and i.p.)

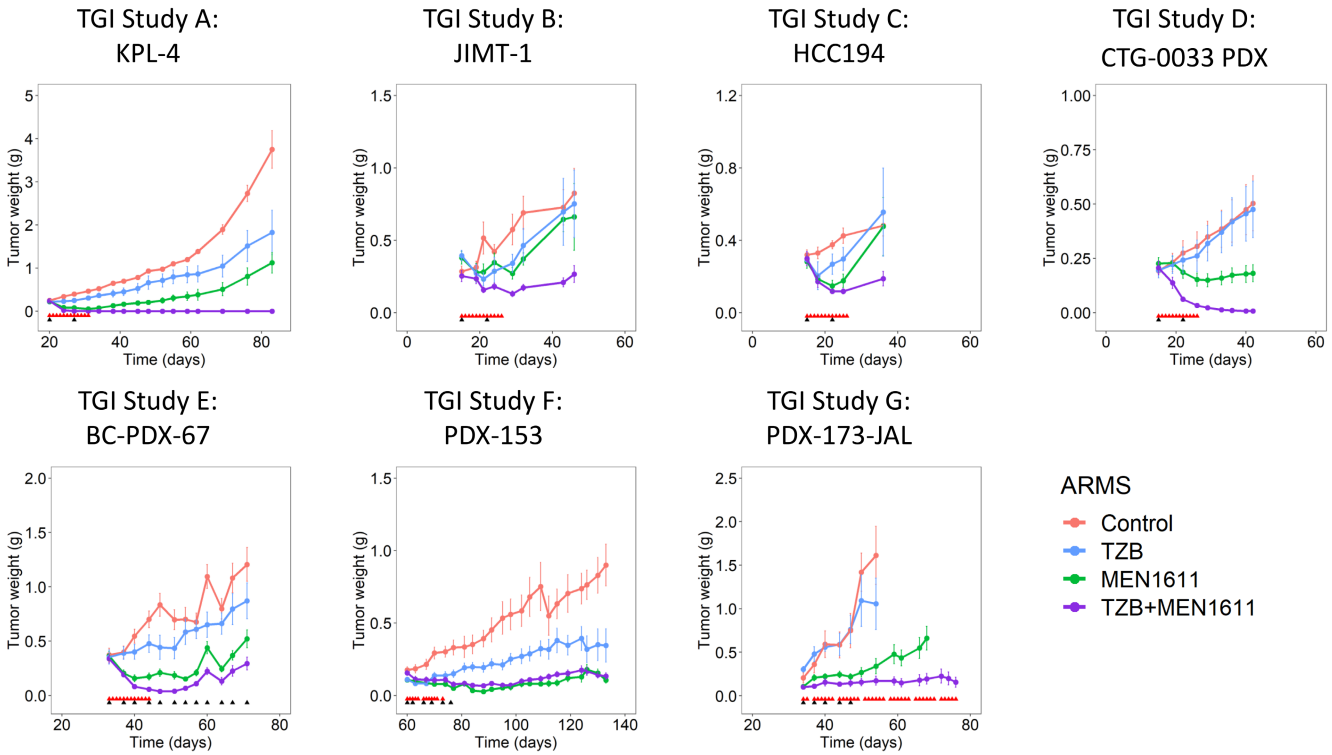

FIGURE 1 Observed mean (±SE) tumor weight profiles stratified by treatment arms and studies. Down-pointing triangles mark dosing events for MEN1611 (red) and TZB (black). TGI, tumor growth inhibition; TZB, trastuzumab.

and MEN1611 (i.v. and p.o.). The PK models were parameterized in terms of F, k_{abs}, CL, V_1, Q, and V_2.

For MEN1611, because bioavailability of solution (*MEN1611-PK study 1*) and suspension (*MEN1611-PK study 2*) were expected to be different (closed to 100% for solution and <100% for suspension), two different F, $F_{solution,}$ and $F_{suspension}$, were estimated.

Pharmacodynamic modeling

TGI model for control and single-agents (TZB and MEN1611) groups

The *Simeoni* TGI model[18] was used to describe the unperturbed tumor growth in control animals and its inhibition after administration of TZB and MEN1611 in monotherapy. The model assumes that, in absence of treatment, tumor follows an exponential + linear growth characterized by rates λ_0 (1/day) and λ_1 (cm^3/day), respectively. In studies where tumor mass did not reach a high volume and the linear phase was not observable, an exponential growth model (reduced *Simeoni* growth model) was used. Under treatment, the model assumes that a fraction of tumor cells, hit by the drug, becomes non-proliferating and enters a mortality chain leading to cell death. Drug-related parameters are the drug potency, $k_{2,TZB}$ and $k_{2,MEN1611}$ (L/μg·day), and the first-order constant describing the kinetics of cell damage and death, $k_{1,TZB}$ and $k_{1,MEN1611}$ (1/day).

Additive 2D-TGI model for co-administration of MEN1611 and TZB (no-interaction hypothesis)

As recommended in refs. 35 and 36, an additive combination model under the hypothesis of no-interaction between TZB and MEN1611 was used to assess the synergism of the combination. This additive 2D-TGI model assumes that TZB and MEN1611 act on tumor cells independently from each other as in monotherapy. Consequently, (i) a cell hit by a drug can be further hit by the other drug, (ii) the whole mortality process is represented by a grid of four by four transit compartments corresponding to all possible damage stages,[24] and (iii) drug-related parameters are the same for the single-agent TGI models.

Synergistic 2D-TGI model for co-administration of MEN1611 and TZB in TZB insensitive PI3K-mutated BC xenograft models

PI3K alterations were reportedly to confer TZB insensitivity to HER2+ BC through a HER2-independent activation of

the PI3K/AkT/mTOR pathway. Therefore, TZB alone was expected to exert no or little anticancer effect (little $k_{2,TZB}$) in PI3K-mutated BC mice models. It was demonstrated that the co-administration of a PI3K inhibitor, such as MEN1611, allows to overcome the TZB insensitivity through the down-regulation of the PI3K/AkT/mTOR pathway.[37]

To model the MEN1611 ability of overcoming TZB insensitivity, it was hypothesized that the PI3K blockage induced by MEN1611 co-administration enhanced the neglectable anticancer activity of TZB on PI3K-mutated BC tumors. In absence of biomarker data quantifying the inhibition of the PI3K/AkT/mTOR pathway, the MEN1611 concentration was used to drive the increase of the TZB activity. The structure of the synergistic 2D-TGI model is like to the additive one except that the TZB-related parameter governing its anticancer effect is increased by a synergistic term proportional to MEN1611 concentration:

$$\frac{dX_{11}(t)}{dt} = \frac{\lambda_0 \cdot X_{11}(t)}{\left[1+\left(\frac{\lambda_0}{\lambda_1}\cdot W(t)\right)^{\psi}\right]^{1/\psi}} - \left(k_{2,MEN1611}C_{MEN1611}(t) + k_{2,TZB,combo}C_{TZB}(t)\right)\cdot X_{11}(t) \quad (2)$$

where $W(t)$ is the tumor weight, $X_{11}(t)$ the proliferating tumor cell compartment and

$$k_{2,TZB,combo} = k_{2,TZB} + k_{2,TZB}\cdot\gamma\cdot C_{MEN1611}(t) \quad (3)$$

with $k_{2,TZB}$ the anticancer potency of TZB in monotherapy and γ the synergistic factor.

Mathematical formulation of the *Simeoni* TGI and the 2D TGI models is reported in Material S3.

Identification of the effective concentration threshold for MEN1611 in combination with TZB in TZB insensitive PI3K-mutated BC xenograft models

A stability analysis of the additive and synergistic 2D-TGI models was performed, under the hypothesis of constant MEN1611 and TZB concentrations ($C_{MEN1611}(t) = C_{MEN1611}$ and $C_{TZB}(t) = C_{TZB}$), in order to identify the minimal effective MEN1611 concentration, $C_{MEN1611,eff}$, able to guarantee tumor eradication when co-administered with TZB in TZB insensitive PI3K-mutated BC xenograft models.[26,38]

From this analysis, it was obtained:

$$C_{MEN1611,eff} = \frac{\lambda_0 - k_{2,TZB}C_{TZB}}{k_{2,MEN1611}} \quad (4)$$

for the additive model, and

$$C_{MEN1611,eff} = \frac{\lambda_0 - k_{2,TZB}C_{TZB}}{k_{2,MEN1611} + \gamma k_{2,TZB}C_{TZB}} \quad (5)$$

for the synergistic model.

Equations 4 and 5 express the threshold concentration of MEN1611 in combination regimen as a function of TZB concentration level. Let $\overline{C_{TZB}}$ be a concentration level of TZB expected to be effective on BC models in absence of resistance. Thus, from Equations 4 and 5 it is possible to derive the corresponding MEN1611 threshold concentration, $C_{MEN1611,eff}(\overline{C_{TZB}})$ that restores the sensitivity to TZB allowing tumor eradication. Consequently, the effectiveness of a given TZB concentration, $\overline{C_{TZB}}$, on a TZB insensitive PI3K-mutated xenograft model can be represented as a function of the co-administered MEN1611 concentration: for $C_{MEN1611} \geq C_{MEN1611,eff}(\overline{C_{TZB}})$ tumor will be eradicated, otherwise tumor will continue to grow (Figure 2).

Extrapolation of effective threshold concentration of MEN1611 in combination with TZB to B-PRECISE-01 patients

To predict a range of MEN1611 concentrations expected to be effective in B-PRECISE-01 patients when combined with TZB, the estimates obtained from preclinical experiments were supposed to be informative for the clinical setting. Because the unbound fraction in plasma of MEN1611 is similar between mouse and human (12.7% and 11.5%, respectively), any correction with protein biding was not needed. Under these assumptions, the minimal effective MEN1611 concentration, $C_{MEN1611,eff}$, was derived from Equations 4 and 5. For this purpose, TZB concentration was supposed constant and fixed to a suitable concentration level, C_{TZB}.

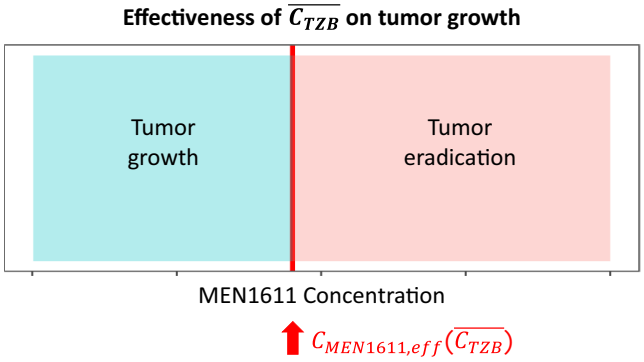

FIGURE 2 Effectiveness of TZB concentration, $\overline{C_{TZB}}$, on growth of TZB insensitive PI3K-mutated BC tumors as a function of MEN1611 concentration. For $C_{MEN1611} \geq C_{MEN1611,eff}(\overline{C_{TZB}})$ tumor will be eradicated (pink area), otherwise tumor will continue to grow (light-blue area). TZB, trastuzumab.

Because information about TZB PK was not available for B-PRECISE-01 patients, TZB concentration levels were derived from steady-state PK parameters reported by the European Medicines Agency (EMA)[39] for three alternative recommended TZB regimens (i.e., i.v. 4 mg/kg loading dose +2 mg/kg q1w [regimen 1], i.v. 8 mg/kg loading dose +6 mg/kg q3w [regimen 2], or s.c. 600 mg q3w [regimen 3]; Table S1 in Material S4). In particular, three different scenarios were considered (Figure 3).

Scenario 1: TZB was supposed equal to the average steady-state concentration, $C_{TZB} = C_{TZB,ss,avg}$, obtained from the median of the exposure during the 21-day treatment period, that is, the area under the curve $\left(AUC_{[0,21day],TZB}\right)$: $C_{TZB,ss,avg} = AUC_{[0,21day],TZB} / 21$.

Scenario 2: The fluctuations of C_{TZB} within the treatment period was accounted for by assuming C_{TZB} equal to the minimum, $C_{TZB,ss,min}$, or maximum, $C_{TZB,ss,max}$, observed concentration in this period. In this way, the worst and best cases were considered.

Scenario 3: The 90% confidence interval (CI) of $AUC_{[0,21day],TZB}$ was considered to account for the inter-patient variability of $C_{TZB,ss,avg}$. The corresponding 90% CI of $C_{TZB,ss,avg}$ was derived and C_{TZB} was supposed to be equal to the 5 degrees or 95 degrees percentile of $C_{TZB,ss,avg}$. Values of C_{TZB} for the scenarios 1–3 are summarized in Table S2 Material S4.

For each TZB administration regimen and each scenario, the full panel of preclinical models was used to derive $C_{MEN1611,eff}$. From these values, the corresponding efficacious MEN1611 exposure between 0–12 h was computed:

$$\text{Effective } AUC_{[0,12h],MEN1611} = 12h \cdot C_{MEN1611,eff}. \quad (6)$$

Data analysis and software

TZB and MEN1611 PK models were developed on average plasma concentration-time profiles from *TZB-PK study 1-2* and *MEN1611-PK study 1-2*, respectively, using a naïve pooled approach. Proportional and combined residual error models ($y = f + (a + b \cdot f) \cdot \varepsilon$ and $y = f + (b \cdot f) \cdot \varepsilon$, where y is the measurement, a and b coefficients, f the model prediction, and ε a standardized random variable normally distributed) were selected for TZB and MEN1611, respectively. The seven in vivo TGI studies were separately analyzed with the following strategy.

TZB and MEN1611 PK models were used to simulate typical plasma concentration-time profiles in input to the PK-PD TGI models for the single-agent and combination groups (no PK interactions were expected during MEN1611 and TZB co-administration).

Tumor-related ($\lambda_0, \lambda_1, W_0$), MEN1611-related ($k_{1,MEN1611}$, $k_{2,MEN1611}$) and TZB-related ($k_{1,TZB}, k_{2,TZB}$) parameters were estimated on data of the control and single-agent arms. In particular, the standard *Simeoni* tumor growth function was used for TGI studies 1 and 6–7, whereas the reduced tumor growth model (i.e., only exponential tumor growth) was adopted in the remaining studies. For TGI studies 1–5, control and treated arms were simultaneously analyzed. For TGI studies 6–7, first the tumor-related parameters were estimated on control groups, then the TZB-related and MEN1611-related parameters were estimated on the corresponding treated arms keeping fixed λ_0, $\lambda_1$to values estimated on control animals. In these cases, a different value of W_0 was estimated for each experimental arm.

For each combination study, the additive 2D-TGI model was used, together with the parameter estimates from control and single-agent arms, to simulate the expected tumor response to the combination regimen under the no-interaction hypothesis. The predicted tumor growth

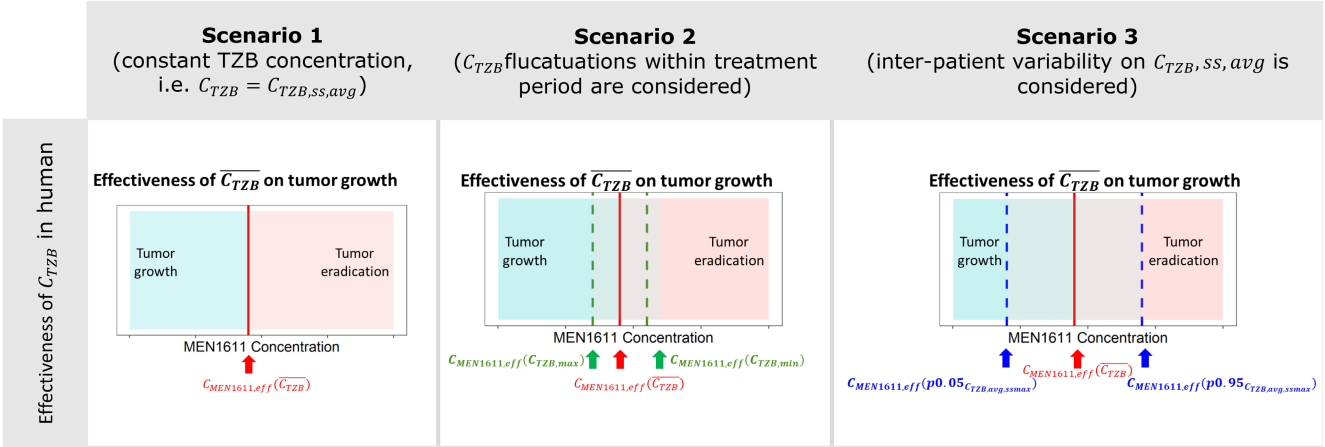

FIGURE 3 Graphical representation of the strategy adopted to extrapolate efficacious $C_{MEN1611}$. $p0.05_{C_{TZB,avg,ss}}$ and $p0.95_{C_{TZB,avg,ss}}$ note the 5 degrees or 95 degrees percentile of $C_{TZB,ss,avg}$, respectively, accounting for interindividual variability. TZB, trastuzumab

curves (PTGCs) were superimposed to TW observed in the combination arms for a visual assessment of drug interactions: experimental TW lying below, above or close to the PTGC indicate a synergistic, antagonistic or no interaction, respectively.[35]

For studies highlighting a synergistic interaction, the synergistic 2D-TGI model was fitted on data from the combination arm to identify the value of the synergistic term γ. In this step, all the other model parameters were fixed to the previous estimates. The root mean squared error on the combination arm was used to quantify the improvement in the goodness-of-fit compared to the additive 2D-TGI model.

A constant residual error model was adopted (i.e., $y = f + a \cdot \varepsilon$).

PK and PK-PD models were implemented and identified in Monolix (version 2016R1; Lixoft, France). Graphical post-processing of data exported from Monolix, model simulations (function "Simulx" of R-package "mlxR"), $C_{MEN1611,eff}$ computations were performed in R (version 3.6.1).

RESULTS

Pharmacokinetic modeling

A two-compartment model with first order absorption and elimination adequately described TZB plasma concentration time courses at the different dose levels after both i.v. and i.p. administrations in tumor-bearing mice of *TZB-PK study 1–2*.

Similarly, the PK model for MEN1611 was successfully identified using concentration-time profiles from *MEN1611-PK study 1–2*. The bioavailability of the solution, $F_{Solution}$, was fixed to 1, whereas the relative bioavailability of suspension, $F_{suspension}$, (*MEN1611-PK study 2*) was estimated on experimental data. The PK model adequately described MEN1611 kinetics after both i.v. and p.o. administrations, following single or multiple dose regimens. The assumption of different bioavailabilities for solution and suspension allowed to describe MEN1611 plasma concentration time courses observed in *MEN1611-PK study 1–2* with the same set of parameters.

For TZB and MEN1611, model parameters were estimated with good precision (relative standard error % < 15%) and goodness-of-fit plots showed that the PK model was unbiased (Figures S8–S13 and Tables S3–S4 in Material S5).

PK/PD modeling of control and single agent arms

For each TGI study, the *Simeoni* TGI model was successfully identified against average TW of control and single-agent treated arms. Fit plots are displayed in Figure 4a for the TGI study A and in Material S6 for the other TGI studies (Figures S14–S17). Parameter estimates are reported in Table 2. Due to data sparseness, some parameter estimates are associated with high uncertainty. Nevertheless, the most impacting parameters (i.e., exponential tumor growth rate λ_0 and drug potencies, $k_{2,TZB}$ and $k_{2,MEN1611}$), were estimated with good precision.

The *Simeoni* tumor growth model or its reduced version were always able to well describe the unperturbed growth in control animals accounting for different growth dynamics characterizing the seven tumor cell lines. In addition, tumor responses to MEN1611 or TZB treatment were well-described by the model that captured the different tumor cell sensitivities to drug treatment. As expected, the *Simeoni* TGI model identified a neglectable anticancer potency of TZB in monotherapy with values of $k_{2,TZB}$ (range = [1.2 E-8, 7.08 E-7] ml·day/ng) significantly lower than estimates obtained on TZB sensitive HER2+ BC xenograft models (see additional data in Material S7).

Assessment of interactions between MEN1611 and TZB

The additive 2D-TGI model together with parameter estimates of Table 2 was used to simulate the expected tumor response to co-administration of MEN1611 and TZB under no-interaction hypothesis. For each study, the obtained PTGC was superimposed on the observed TWs of the combination arm (Figure 4b, and Figure S18 Material S6). Experimental data from TGI studies 1–5 lied below the PTGC highlighting that MEN1611 with TZB co-administration resulted in a greater effect than that predicted by the additive 2D-TGI model ("synergistic" effect). In contrast, there were not significant differences between observed and predicted TW in TGI studies 6–7. Therefore, for PDX-153 and PDX-173-JAL models the combination of MEN1611 and TZB did not exert an anticancer effect more than additive.

Synergistic 2D-TGI model for the combination of MEN1611 and TZB in TZB insensitive PI3K-mutated BC xenograft models

The synergistic 2D-TGI model was separately fitted on TW data from the combination arms highlighting a synergistic interaction between MEN1611 and TZB (TGI studies 1–5). The synergistic factor, γ, was estimated with good

TABLE 2 Model parameter estimates obtained on control and single-agent treated arms

Study	Tumor line	λ_0 (1/day)	λ_1 (cm^3/day)	W_0 (g)	$k_{1,TZB}$ (1/day)	$k_{2,TZB}$ (ml·day/ng)	$k_{1,MEN1611}$ (1/day)	$k_{2,MEN1611}$ (ml·day/ng)	γ (–)
Study A	KPL4	0.043 (2%)	0.496 (>100%)	0.106 (7%)	5.1 (42%)	1.78 e-7 (17%)	9.77 (43%)	2.01 e-4 (12%)	0.0425 (2%)
Study B	JIMT1	0.035 (11%)	–	0.177 (13%)	5.36 (>100%)	9.92 e-8 (93%)	99.7 (85%)	9.21 e-5 (45%)	0.0307 (10%)
Study C	HCC194	0.038 (19%)	-	0.137 (19%)	84.5 (>100%)	1.2 E-8 (>100%)	55.1 (>100%)	1.13 E-4 (>100%)	0.263 (23%)
Study D	CTG-0033	0.032 (4%)	–	0.129 (5%)	88.4 (>100%)	2.28 E-8 (>100%)	3.82 (>100%)	2.71 E-4 (5%)	0.344 (10%)
Study E	BC-PDX-67	0.032 (7%)	–	0.125 (13%)	3.13e3 (>100%)	1.63 e-7 (22%)	20.9 (>100%)	3.39 e-4 (12%)	0.024 (37%)
Study F	PDX-153	0.025 (8%)	0.011 (5%)	Control: 0.04 (17%) TZB: 0.025 (15%) MEN1611: 0.024 (14%)	1.1 (100%)	1.98 e-7 (41%)	1.01 (6%)	4.56 E-4 (11%)	–
Study G	PDX-173-JAL	0.102 (22%)	0.108 (28%)	Control: 0.007 (100%) TZB: 0.01 (15%) MEN1611: 0.004 (10%)	1.03 (>100%)	8888 (30%)	79.4 (>100%)	2.57 E-4 (5%)	–

Abbreviation: TZB, Trastuzumab.

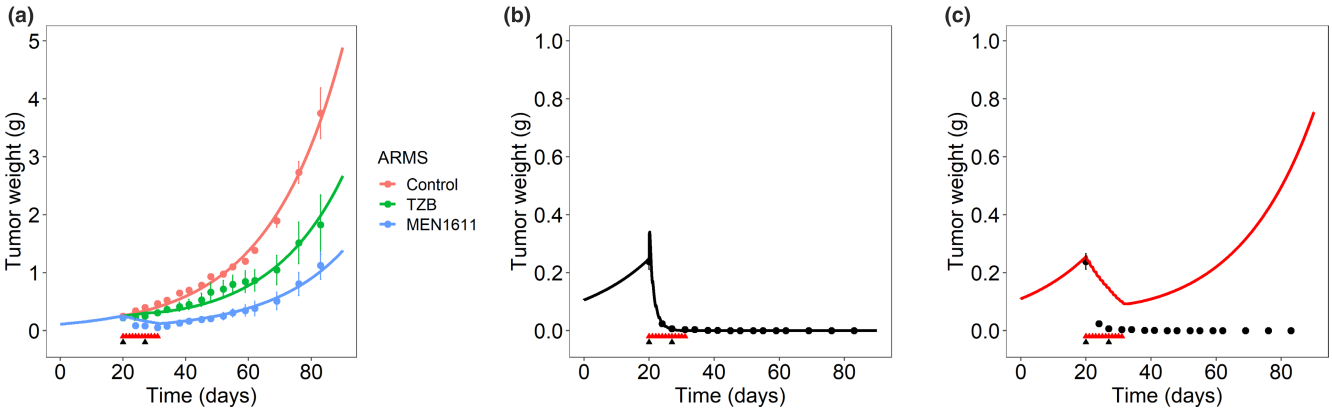

FIGURE 4 Results for the *TGI* study A: (a) Observed (dots) and model-predicted (solid lines) tumor weight in control and single-agent treated groups. (b) Predicted tumor growth curves (PTGCs) obtained by the Additive 2D-TGI model (red lines) were superimposed on the experimental data (black dots) for combination arm. Data lying below the PTGC highlighted a synergistic effect of the combination. (c) Observed (dots) tumor weight in the combination arm together with predictions by the Synergistic 2D-TGI model (solid line). In all the panels, vertical bars show ± standard error of the data. Down-pointing triangles mark dosing events for MEN1611 (red) and TZB (black). TGI, tumor growth inhibition; TZB, trastuzumab.

precision, keeping fixed the other model parameters to previous estimates (Table 2).

In all cases, the introduction of the synergistic interaction enabled the model to well capture the enhanced TGI observed in the combination arm (Figure 4c and Figures S19–S22 Material S6), significantly improving the goodness of fit compared the additive 2D-TGI model (see RMSE reported in Table S5).

Extrapolation to human (B-PRECISE-01 patient population) of the effective MEN1611 concentration threshold in combination with TZB

Equations 4 and 5 together with parameter estimates obtained from the preclinical experiments (Table 2) were used to identify a set of minimal MEN1611 concentrations

expected to be effective in B-PRECISE-01 patients when co-administrated with TZB at clinical recommended doses. From the estimated $C_{MEN1611,eff}$, the ranges of minimal effective $AUC_{[0,12h],MEN1611}$ were computed. Results were reported in Table 3 for the TZB regimen 1 and in Tables S6–S7 Material S8 for regimens 2–3.

For regimen 1, in which TZB was given q1w, the fluctuations of TZB concentrations within the dosing interval (21 days) were limited (scenario 2). Therefore, TZB concentration could be considered approximately constant and the range width of the minimal effective $AUC_{[0,12h],MEN1611}$ was driven by the high TZB inter-patient variability (scenario 3). For regimens 2–3 in which TZB was administered q3w, fluctuations of TZB concentrations (scenario 2) were more significant. Nevertheless, the interpatient variability remained the most impactful source of variability in determining the MEN1161 effective threshold concentration.

When TZB is administered following regimen 1, considering the whole panel of the PIK3CA mutated tumor cell lines (exclusion of PDX173JAL) and the TZB variability, a range of effective exposure for MEN1611 (155–2202 ng·h/ml) was predicted. Thus, MEN1611 and TZB combination was expected to be effective in the vast majority of patients with $AUC_{[0,12h],MEN1611}$ higher than 2000 ng·h/ml. A similar threshold was predicted for the alternative i.v. regimen of TZB (regimen 2). A slightly lower effective exposure ($AUC_{[0,12h],MEN1611}$ ~1500 ng·h/ml) was predicted in patients treated with TZB s.c. 600 mg q3w (regimen 3).

DISCUSSION

In this work, a translational modeling approach was applied to determine a minimum target exposure of MEN1611, a novel orally bioavailable PI3K inhibitor in clinical development, when given in combination with TZB to treat patients with HER2+ PIK3CA-mutated advanced/metastatic BC insensitive to TZB.

A stepwise modeling approach was carried out. First, the preclinical TZB and MEN1611 PK were characterized using plasma concentration time courses in tumor-bearing and tumor-free mice, respectively. The PKs of both drugs was well described by a two-compartment model with first order absorption and elimination. No PK interaction was expected and modeled between these two drugs.

Second, a PK-PD model was developed to describe the relationship between MEN1611 exposure in plasma and the anticancer activity exerted when given in combination with TZB. Seven combination studies in cell-derived and patient-derived xenograft models representative of human HER2+ BC nonresponsive to TZB and harboring PI3K/AKT/mTOR pathway alterations were analyzed. The *Simeoni* TGI model[18] successfully characterized tumor growth dynamics in control and single-agent treated arms identifying a neglectable anticancer activity for TZB in monotherapy. Starting from the *Simeoni* TGI model, an ad hoc combination PK-PD model was developed to describe tumor growth in combination arms. Accounting for MEN1611 ability to restore TZB activity on tumor cells, the proposed synergistic 2D-TGI model was able to capture the synergism of the combination, as observed in most of the experiments.

Third, a mathematical analysis of the combination models was performed to develop a mathematical tool that, for each given TZB concentration level expected to be effective in absence of resistance, predicts the minimum MEN1611 concentration able to guarantee tumor eradication also in TZB insensitive xenograft mice.

Finally, mathematical relationships (Equations 4 and 5) derived from the xenograft models were used to extrapolate the effective MEN1611 exposures to human. For that respect, it was assumed that total MEN1611 concentration can be used in both mice and human as MEN1611 unbound fraction in plasma is similar in mouse and human: 12.7% and 11.5%, respectively. Three alternative TZB administration regimens were considered: (i) i.v. 4 mg/kg loading dose +2 mg/kg q1w, (ii) i.v. 8 mg/kg loading dose +6 mg/kg q3w, or (iii) s.c. 600 mg q3w. For each regimen, typical steady-state TZB plasma level in patients with BC, together with its intrapatient fluctuations and interpatient variability, was used to predict a range of minimum

TABLE 3 Effective MEN1611 exposures ($AUC_{[0,12h],MEN1611}$) in B-PRECISE patients receiving TZB i.v. 4 mg/kg + 2 mg/kg q1w (TZB regimen 1) from a panel of breast cancer tumor lines

	$AUC_{[0,12h],MEN1611}$ (ng·day/ml)						
Cancer model	**KPL4**	**JIMT1**	**HCC194**	**CTG003**	**BC-PDX-67**	**PDX-153**	**PDX-173-JAL**
Scenario 1: $C_{TZB} = C_{TZB,ss,avg}$	359	946	1152	406	341	239	2071
Scenario 2: fluctuations of C_{TZB} within the treatment period	[241, 486]	[697, 1209]	[934, 1379]	[326, 488]	[230, 444]	[106, 334]	[1225, 2677]
Scenario 3: Inter-patient variability on $C_{TZB,ss,avg}$	[171, 999]	[545, 2187]	[800, 2202]	[277, 783]	[155, 737]	[0, 519]	[488, 3847]

Abbreviation: TZB, trastuzumab.

effective MEN1611 exposures for B-PRECISE patients. When TZB was administered i.v. (i.e., regimens 1 and 2), a MEN1611 $AUC_{[0,12h],ss}$ higher than 2000 ng·h/ml was expected to be associated with a high likelihood of effective antitumor activity in the vast majority of patients. A slightly lower exposure (i.e., −25%) was predicted for the TZB administered q3w s.c. schedule. These concentration thresholds accounted for the whole panel of tumor cell lines harboring PIK3CA mutations as well as for the fluctuations within treatment period and interpatient variability of the co-administered TZB exposure. However, also considering the preclinical model PDX173JAL that harbors a different PI3K/AkT/mTOR pathway (PIK3CG mutation), such levels of MEN1611 exposures were expected to be effective in patients with an equal or higher TZB exposure than typical.

Model predicted ranges of active MEN1611 exposures were integrated with PKs and safety data from the FIH study[11] to verify if clinically relevant antitumor activity could be expected at safe MEN1611 doses. The steady-state exposures of MEN1611 reached at MTD (48 mg b.i.d.) was consistent with the ranges of exposures identified as most likely effective in patients with HER2+ PIK3CA mutated BC in combination with TZB, confirming the adequacy of the administered protocol proposed for the phase Ib B-PRECISE-01. Model-based predictions were first confirmed by the promising antitumor activity observed in patients receiving MEN1611 at 16, 32, and 48 mg b.i.d. in combination with weekly i.v. infusions of TZB during the dose escalation cohort of the B-PRECISE-01 study.[40] This provided the rationale for the subsequent expansion cohort at 48 mg b.i.d. that was selected as the recommended phase II dose of MEN1611 in combination with TZB. Preliminary results of the interim analysis of the expansion cohort further confirmed the model predicted range of effective MEN1611 exposures for B-PRECISE patients.[41] Indeed, significant antitumor activity together with prolonged disease control was observed in patients receiving MEN1611 doses able to reproduce systemic exposures fully inside the range of concentrations expected to be effective in patients with HER2+ PI3KCA-mutated BC when combined with TZB.

Overall, the present work highlights the critical contribution of modeling approaches using nonclinical data to inform potential effective drug exposures in patients. The predicted effectiveness is clearly based only on the expected antitumor activity and does not consider the global patient benefits (i.e., manageable adverse events, long term efficacy, etc). However, preclinical predictions of clinically active exposures can be integrated with preliminary PK and safety data from the FIH studies, when available, allowing an early assessment of an adequate therapeutic window and of clinical doses and protocols able to ensure a good efficacy-safety profile.

In the case of TZB and MEN1611 combination, predictions of target exposures were based on a PK-PD modeling of preclinical data under some specific hypothesis. First, available MEN1611 PK data in tumor-bearing mice (data not shown) were poorly informative. Because there is no strong evidence of differences between MEN1611 PK in tumor-free and tumor-bearing mice, the PK model was developed on data from tumor-free mice. In contrast, differences between tumor-free and tumor-bearing mice were observed in PK TZB for which a PK model was developed on literature data from tumor-bearing mice as no in house TZB PK data were available. Second, available TGI studies included groups of murine animals treated with MEN1611 and TZB given alone or in combination at a single dose level. For both monotherapy and combination regimens, the anticancer drug effect could be linearly dependent on plasma concentration and mainly driven by AUC. No information on target-engagement and markers of pathway inhibition (e.g., pS6 or pAKT) were available. Nevertheless, if future experiments provide data on robust biomarkers of pharmacological activity, their integration will likely strengthen the translational modeling approach.[42–44] Third, in the synergistic model the restoration of TZB anticancer potency was linearly driven by MEN1611 concentration due to the lack of data that could support the development of more complex models accounting, for example, for a saturation of the restoration process. This could lead to bias in the extrapolations of restored TZB potency at significantly higher MEN1611 concentrations. However, at the MEN1611 concentration levels reached in the analyzed combination TGI studies, the restored TZB potency assumed reasonable values that resulted consistent with estimates obtained on TZB sensitive BC models (see Material S7). The use of human equivalent dose for MEN1611 guaranteed that also extrapolations to human were unbiased. Finally, the extrapolation of the effective MEN1611 exposures from mice to humans was based on total plasma concentration without applying any plasma protein biding correction between mice and humans. In the case of MEN1611, this choice was justified by the strong similarity between the unbound fractions in mice and humans. However, in a different scenario with relevant interspecies differences, free, rather than total, concentration, should have been used in the extrapolation.[29]

The current analysis stressed on some more general considerations for translational modeling. First of all, mathematical models to be used for translational purpose should be based on reliable preclinical data from in vivo animal models representative of the target patient population. For the MEN1611 and TZB combination, six xenograft models involving HER2+ PIK3CA-mutated TZB insensitive BC cell lines were selected as representative of the B-PRECISE-01 patient population. They

included standardized human cell lines (KPL-4, JIMT1, and HCC194) and patient-derived cell lines (CTG003, BC-PDX-67, and PDX-153) that are generally considered more representative of patient tumor characteristics and clinical responses. In addition, TGI study G involving the PDX-173-JAL model, representative of the HER2+, ER+, and TZB-resistant BC harboring a different PI3K pathway alteration (mutated PIK3CG gene), was considered for a proof-of-concept of restoration of the TZB resistance by the co-treatment with MEN1611. Interestingly, the PDX-173-JAL model provided the highest model estimates of effective MEN1611 exposures. Moreover, the clinical predictivity of the preclinical results was maximized by the use of clinically relevant doses obtained through a back translation of expected human exposures into mice.[45,46]

Further, translational quantitative approaches should rely on mathematical models with mechanistic basis. Here, a 2D-TGI model for TZB and MEN1611 combination was developed starting from the semi-mechanistic *Simeoni* TGI model which provides estimates of drug activity with demonstrated translatability.[28,29] Moreover, synergistic (or antagonist) interactions of co-administered drugs should be adequately incorporated in the modeling framework, acknowledging that required exposure in combination for enhanced (or reduced) efficacy may be different from the required exposure for single agent efficacy. For MEN1611 and TZB combination, an adequate modeling of the observed synergism significantly impacted the predicted human effective MEN1611 exposures. If model predictions were performed overlooking the drug synergism, a much higher MEN1611 exposure would have been expected to be effective in patients.

Finally, translational approaches intending to make robust clinical inferences from preclinical data might not provide a point-estimate of effective clinical exposure. Indeed, the various sources of variability should be accounted for during "bench-to-bed-side" extrapolations. For MEN1611 and TZB combination, a range of MEN1611 effective exposures, instead of a single value, was derived from a panel of tumor cell lines associated with different growth patterns as well as different degrees of MEN1611 sensitivity. In addition, because MEN1611 efficacy was significantly affected by the TZB co-administration schedules, three possible alternative TZB regimens were considered. For each of them, observed fluctuations and interpatient variability in TZB exposure were taken into account in the prediction of effective exposures of MEN1611. Interpatient variability of TZB exposure was found to highly affect the minimum effective MEN1611 exposure and should be adequately considered.

CONCLUSIONS

A translational PK-PD modeling framework was developed in order to predict a range of minimum target exposures to be attained for MEN1611, when administered in combination with TZB in patients with HER2+ PIK3CA-mutated BC from a panel of xenograft experiments. A threshold for MEN1611 exposure associated with a high likelihood of effective antitumor activity was identified for three alternative administration schedules of TZB. The results of the analysis confirmed the adequacy of the dose administered in the phase Ib B-PRECISE-01 study in patients with HER2+ advanced/metastatic PIK3CA-mutated BC.

Translational approaches based on the PK-PD modeling of preclinical data confirmed to be useful tools to anticipate effective exposures in human informing the identification of pharmacologically active doses in clinical trials of combination anticancer therapies.

AUTHOR CONTRIBUTIONS

E.M.T. and P. Magni wrote the manuscript. E.B., C.P., S.B., and P. Mazzei designed the research. A.F. and G.M. performed the research. E.M.T. and P.M. analyzed the data. E.M.T. and P. Mazzei contributed new analytical tools.

FUNDING INFORMATION

No funding was received for this work.

CONFLICT OF INTEREST

E.B., C.P., S.B., G.M., A.F., and P.Mazzei are Menarini employees. E.M.T. and P.Magni are employees of Università Degli Studi Di Pavia.

ORCID

Alessio Fiascarelli https://orcid.org/0000-0002-7453-4262
Paolo Magni https://orcid.org/0000-0002-8931-4676

REFERENCES

1. Slamon DJ, Clark GM, Wong SG, Levin WJ, Ullrich A, McGuire WL. Human breast cancer: correlation of relapse and survival with amplification of the HER-2/neu oncogene. *Science (80-).* 1987;235:177-182.
2. Carey LA, Perou CM, Livasy CA, et al. Race, breast cancer subtypes, and survival in the Carolina breast cancer study. *JAMA.* 2006;295(21):2492-2502.
3. Kreutzfeldt J, Rozeboom B, Dey N, De P. The trastuzumab era: current and upcoming targeted HER2+ breast cancer therapies. *Am J Cancer Res.* 2020;10(2):1045.
4. Wilks ST. Potential of overcoming resistance to HER2-targeted therapies through the PI3K/Akt/mTOR pathway. *Breast.* 2015;24(5):548-555.

5. Rexer BN, Arteaga CL. Intrinsic and acquired resistance to HER2-targeted therapies in HER2 gene-amplified breast cancer: mechanisms and clinical implications. *Crit Rev Oncog*. 2012;17(1):1-16.
6. Vu T, Claret FX. Trastuzumab: updated mechanisms of action and resistance in breast cancer. *Front Oncol*. 2012;2:62.
7. Cidado J, Park BH. Targeting the PI3K/Akt/mTOR pathway for breast cancer therapy. *J Mammary Gland Biol Neoplasia*. 2012;17(3):205-216.
8. Vanhaesebroeck B, Perry MWD, Brown JR, André F, Okkenhaug K. PI3K inhibitors are finally coming of age. *Nat Rev Drug Discov*. 2021;20(20):741-769.
9. Ohwada J, Ebiike H, Kawada H, et al. Discovery and biological activity of a novel class i PI3K inhibitor, CH5132799. *Bioorg Med Chem Lett*. 2011;21(6):1767-1772.
10. Tanaka H, Yoshida M, Tanimura H, et al. The selective class I PI3K inhibitor CH5132799 targets human cancers harboring oncogenic PIK3CA mutations. *Clin Cancer Res*. 2011;17(10):3272-3281.
11. Blagden S, Olmin A, Josephs D, et al. First-in-human study of CH5132799, an oral class I PI3K inhibitor, studying toxicity, pharmacokinetics, and pharmacodynamics, in patients with metastatic cancer. *Clin Cancer Res*. 2014;20(23):5908-5917.
12. Fiascarelli A, Merlino G, Capano S, et al. Characterization of the mechanism of action and efficacy of MEN1611 (PA799), a novel PI3K inhibitor, in breast cancer preclinical models. *Ann Oncol*. 2019;30:v781-v782.
13. Piccart-Gebhart MJ, Aftimos PG, Duhoux FP, et al. B-PRECISE-01 study: a phase Ib trial of MEN1611, a PI3K inhibitor, combined with trastuzumab ± fulvestrant for the treatment of HER2-positive advanced or metastatic breast cancer. *J Clin Oncol*. 2019;37(15):TPS1101.
14. Bonate PL. Modeling tumor growth in oncology. In: Bonate PL, Howard DR\, eds. *Pharmacokinetics in Drug Development*. Springer; 2011:1-19.
15. Wang Z, Deisboeck TS. Mathematical modeling in cancer drug discovery. *Drug Discov Today*. 2014;19(2):145-150.
16. Zhang P, Brusic V. Mathematical modeling for novel cancer drug discovery and development. *Expert Opin Drug Discovery*. 2014;9(10):1133-1150.
17. Carrara L, Lavezzi SM, Borella E, De Nicolao G, Magni P, Poggesi I. Current mathematical models for cancer drug discovery. *Expert Opin Drug Discovery*. 2017;12(8):785-799.
18. Simeoni M, Magni P, Cammia C, et al. Predictive pharmacokinetic pharmacodynamic modeling tumor growth kinetics xenograft model after administration AntiCancer agents. *Cancer Res*. 2004;64:1094-1101.
19. Terranova N, Tosca EM, Pesenti E, Rocchetti M, Magni P. Modeling tumor growth inhibition and toxicity outcome after administration of anticancer agents in xenograft mice: a dynamic energy budget (DEB) approach. *J Theor Biol*. 2018;450:1-14.
20. Tosca EM, Pigatto MC, Dalla Costa T, Magni P. A population dynamic energy budget-based tumor growth inhibition model for etoposide effects on Wistar rats. *Pharm Res*. 2019;36(3):38.
21. Tosca EM, Rocchetti M, Pesenti E, Magni P. A tumor-in-host DEB-based approach for modeling cachexia and bevacizumab resistance. *Cancer Res*. 2020;80(4):820-831.
22. Tosca EM, Rocchetti M, Magni P. A dynamic energy budget (DEB) based modeling framework to describe tumor-in-host growth inhibition and cachexia onset during anticancer treatment in in vivo xenograft studies. *Oncotarget*. 2021;12(14):1434-1441.
23. Tosca EM, Rocchetti M, Pesenti E, Magni P. Modeling resistance development to bevacizumab in xenograft experiments by coupling hypoxia-mediated mechanism and a dynamic energy budget (DEB) based tumor-in-host model. *J Pharmacokinet Pharmacodyn*. 2018;45:S25-S26.
24. Terranova N, Germani M, Del Bene F, Magni P. A predictive pharmacokinetic-pharmacodynamic model of tumor growth kinetics in xenograft mice after administration of anticancer agents given in combination. *Cancer Chemother Pharmacol*. 2013;72(2):471-482.
25. Rocchetti M, Germani M, Del Bene F, et al. Predictive pharmacokinetic--pharmacodynamic modeling of tumor growth after administration of an anti-angiogenic agent, bevacizumab, as single-agent and combination therapy in tumor xenografts. *Cancer Chemother Pharmacol*. 2013;71(5):1147-1157.
26. Cardilin T, Almquist J, Jirstrand M, et al. Tumor static concentration curves in combination therapy. *AAPS J*. 2017;19(2):456-467.
27. Tosca EM, Gauderat G, Fouliard S, Burbridge M, Chenel M, Magni P. Modeling restoration of gefitinib efficacy by co-administration of MET inhibitors in an EGFR inhibitor-resistant NSCLC xenograft model: a tumor-in-host DEB-based approach. *CPT Pharmacometrics Syst Pharmacol*. 2021;10(11):1-16.
28. Rocchetti M, Simeoni M, Pesenti E, De Nicolao G, Poggesi I. Predicting the active doses in humans from animal studies: a novel approach in oncology. *Eur J Cancer*. 2007;43(12):1862-1868.
29. Tosca EM, Terranova N, Stuyckens K, et al. A translational model-based approach to inform the choice of the dose in phase 1 oncology trials: the case study of erdafitinib. *Cancer Chemother Pharmacol*. 2021;89(11):117-128.
30. Venkatakrishnan K, Friberg LE, Ouellet D, et al. Optimizing oncology therapeutics through quantitative translational and clinical pharmacology: challenges and opportunities. *Clin Pharmacol Ther*. 2015;97(1):37-54.
31. Pastuskovas CV, Mundo EE, Williams SP, et al. Effects of anti-VEGF on pharmacokinetics, biodistribution, and tumor penetration of trastuzumab in a preclinical breast cancer model. *Mol Cancer Ther*. 2012;11(3):752-762.
32. Palm S, Enmon RM, Matei C, et al. Pharmacokinetics and biodistribution of 86Y-trastuzumab for 90Y dosimetry in an ovarian carcinoma model: correlative MicroPET and MRI. *J Nucl Med*. 2003;44(7):1148-1155.
33. Tomayko MM, Reynolds CP. Determination of subcutaneous tumor size in athymic (nude) mice. *Cancer Chemother Pharmacol*. 1989;24(3):148-154.
34. Euhus DM, Hudd C, Laregina MC, Johnson FE. Tumor measurement in the nude mouse. *J Surg Oncol*. 1986;31(4):229-234.
35. Rocchetti M, Del Bene F, Germani M, et al. Testing additivity of anticancer agents in pre-clinical studies: a PK/PD modelling approach. *Eur J Cancer [Internet]*. 2009;45(18):3336-3346. doi:10.1016/j.ejca.2009.09.025
36. Magni P, Terranova N, Del Bene F, Germani M, De Nicolao G. A minimal model of tumor growth inhibition in combination regimens under the hypothesis of no interaction between drugs. *IEEE Trans Biomed Eng*. 2012;59(8):2161-2170.

37. Burris HA. Overcoming acquired resistance to anticancer therapy: focus on the PI3K/AKT/mTOR pathway. *Cancer Chemother Pharmacol*. 2013;71(4):829-842.
38. Magni P, Simeoni M, Poggesi I, Rocchetti M, De Nicolao G. A mathematical model to study the effects of drugs administration on tumor growth dynamics. *Math Biosci*. 2006;200(2):127-151.
39. European Environment Agency (EEA). Herceptin: EPAR, product information. 2019; 53: 1689–99.https://www.ema.europa.eu/en/documents/product-information/herceptin-epar-product-information_it.pdf
40. Piccart M, Borrego MR, Duhoux F, et al. Results of the phase Ib dose escalation study of MEN1611, a PI3K inhibitor, combined with trastuzumab (T) ± fulvestrant (F) for HER2+/PIK3CA mutant (Mut) advanced or metastatic (a/m) breast cancer (BC). *Ann Oncol*. 2020;31:S386.
41. Piccart M, Ruiz Borrego M, Arkenau H-T, et al. MEN1611, a PI3K inhibitor, combined with trastuzumab (T) ± fulvestrant (F) for HER2+/PIK3CA mutant (Mut) advanced or metastatic (a/m) breast cancer (BC): safety and efficacy results from the ongoing phase Ib study (B-PRECISE-01). *Ann Oncol*. 2021;32:S478-S479.
42. Bueno L, de Alwis DP, Pitou C, et al. Semi-mechanistic modelling of the tumour growth inhibitory effects of LY2157299, a new type I receptor TGF-β kinase antagonist, in mice. *Eur J Cancer*. 2008;44(1):142-150.
43. Salphati L, Wong H, Belvin M, et al. Pharmacokinetic-pharmacodynamic modeling of tumor growth inhibition and biomarker modulation by the novel phosphatidylinositol 3-kinase inhibitor GDC-0941. *Drug Metab Dispos*. 2010;38(9):1436-1442.
44. Ribba B, Watkin E, Tod M, et al. A model of vascular tumour growth in mice combining longitudinal tumour size data with histological biomarkers. *Eur J Cancer*. 2011;47(3):479-490.
45. Liston DR, Davis M. Clinically relevant concentrations of anticancer drugs: a guide for nonclinical studies. *Clin Cancer Res*. 2017;23(14):3489-3498.
46. Spilker ME, Chen X, Visswanathan R, et al. Found in translation: maximizing the clinical relevance of nonclinical oncology studies. *Clin Cancer Res*. 2017;23(4):1080-1090.

SUPPORTING INFORMATION

Additional supporting information can be found online in the Supporting Information section at the end of this article.

How to cite this article: Tosca EM, Borella E, Piana C, et al. Model-based prediction of effective target exposure for MEN1611 in combination with trastuzumab in HER2-positive advanced or metastatic breast cancer patients. *CPT Pharmacometrics Syst Pharmacol*. 2023;12:1626-1639. doi:10.1002/psp4.12910